Radiation Dosimetry for ^{90}Y-2IT-BAD-Lym-1 Extrapolated from Pharmacokinetics Using ^{111}In-2IT-BAD-Lym-1 in Patients with Non-Hodgkin's Lymphoma

Gerald L. DeNardo, Robert T. O'Donnell, Sui Shen, Linda A. Kroger, Aina Yuan, Claude F. Meares, David L. Kukis, and Sally J. DeNardo

Department of Internal Medicine, University of California Davis Medical Center, Sacramento; and Department of Chemistry, University of California Davis, Davis, California

Several monoclonal antibodies, including Lym-1, have proven effective for treatment of hematologic malignancies. Lym-1, which preferentially targets malignant lymphocytes, has induced therapeutic responses and prolonged survival in patients with non-Hodgkin's lymphoma (NHL) when labeled with ^{131}I. Because radiometal-labeled monoclonal antibodies provide higher tumor radiation doses than corresponding ^{131}I-labeled monoclonal antibodies, the radiation dosimetry of ^{90}Y-2-iminothiolane-2-[p-(bromoacetamido)benzyl]-1,4,7,10-tetraazacyclododecane-*N,N',N'',N'''*-tetraacetic acid-Lym-1 (^{90}Y-2IT-BAD-Lym-1) is of importance because of its potential for radioimmunotherapy. Although ^{90}Y has attractive properties for therapy, its secondary bremsstrahlung is less suitable for imaging and pharmacokinetic studies in patients. Thus, the pharmacokinetic data obtained for ^{111}In-2IT-BAD-Lym-1 in patients with NHL were used to calculate dosimetry for ^{90}Y-2IT-BAD-Lym-1. **Methods:** Thirteen patients with advanced-stage NHL were given a preload dose of unmodified Lym-1 followed by an imaging dose of ^{111}In-2IT-BAD-Lym-1. Sequential imaging and blood and urine samples obtained for up to 10 d after infusion were used to assess pharmacokinetics. Using ^{111}In pharmacokinetic data and ^{90}Y physical constants, radiation dosimetry for ^{90}Y-2IT-BAD-Lym-1 was determined. **Results:** The uptake of ^{111}In-2IT-BAD-Lym-1 in tumors was greater than uptakes in the lung and kidney but similar to uptakes in the liver and spleen. The biologic half-time in tumors was greater than in lungs. The mean radiation dose to tumors was 6.57 ± 3.18 Gy/GBq. The mean tumor-to-marrow (from blood) radiation ratio was 66:1, tumor-to-total body was 13:1, and tumor-to-liver was 1:1. Images of ^{111}In were of excellent quality; tumors and normal organs were readily identified. Mild and transient Lym-1 toxicity occurred in 3 patients. **Conclusion:** Because of the long residence time of ^{111}In-2IT-BAD-Lym-1 in tumors, high ^{90}Y therapeutic ratios (tumor-to-tissue radiation dose) were achieved for some tissues, but the liver also showed high uptake and retention of the radiometal.

Key Words: antibody; radioimmunotherapy; radiation dosimetry; pharmacokinetics; ^{90}Y

J Nucl Med 2000; 41:952–958

Received May 3, 1999; revision accepted Sep. 14, 1999.

For correspondence or reprints contact: Gerald L. DeNardo, MD, Molecular Cancer Institute, Section of Radiodiagnosis and Therapy, 1508 Alhambra Blvd., Ste. 3100, Sacramento, CA 95816.

Monoclonal antibodies (MAbs) labeled with ^{131}I have proven effective for radioimmunotherapy (RIT) of hematologic malignancies but less so for solid tumors (*1*). ^{90}Y is an attractive radionuclide for RIT because of the range and energy of its β emissions; absence of γ emissions, allowing outpatient RIT; and ready availability at moderate cost. Its half-time is suitable to the uptake and residence time of many MAbs in tumors. Clinical trials of RIT using ^{90}Y-labeled MAbs in hematologic malignancies (*2–8*) and solid tumors (*9–13*) have been encouraging. Although ^{90}Y has favorable characteristics for therapy, its lack of a γ photopeak has led many to use ^{111}In as a surrogate tracer. To conjugate ^{90}Y for RIT, the macrocyclic chelating agent 1,4,7,10-tetraazacyclododecane-*N,N',N'',N'''*-tetraacetic acid (DOTA) (*14*) was developed and has been shown to provide stable radiopharmaceuticals of ^{90}Y and ^{111}In (*15*). Because ^{131}I-Lym-1 has been shown effective in non-Hodgkin's lymphoma (NHL), and radiometals are retained longer in tumors than corresponding radioiodinated MAbs, the radiation dosimetry for ^{90}Y-2-iminothiolane-2-[p-(bromoacetamido)benzyl]-DOTA-Lym-1 (^{90}Y-2IT-BAD-Lym-1) was calculated using the pharmacokinetics of ^{111}In-2IT-BAD-Lym-1 obtained in patients with NHL.

MATERIALS AND METHODS

Patient Population

Thirteen patients (10 men, 3 women; age range, 33–71 y; mean age, 51 y) with advanced B-cell NHL were enrolled in the study (Table 1). According to the Working Formulation of NHL for Clinical Usage (*16*), 2 patients had low-grade, 7 had intermediate-grade, and 4 had high-grade lymphoma. Lym-1 reactivity was documented on 10 of the patients by immunohistochemical staining and on 3 by imaging. All patients, except 1, had quantifiable tumors, including at least 1 tumor of ≥2-cm diameter. One patient had undergone splenectomy, 5 others had enlarged spleens, and 1 patient had evidence of circulating malignant cells reactive with Lym-1. Three patients had marrow NHL documented by biopsy to be <25% of the cellular marrow elements in each instance. Mean

TABLE 1
Synopsis of Data of 13 Patients Given ^{111}In-2IT-BAD-Lym-1

Patient	Age (y)	Sex	Histology	Ann Arbor stage	Body weight (kg)	Blood volume (L)	Lym-1 (mg)
1	61	M	I (DL)	3	62	4.1	30
2	33	M	H (LCI)	4	79	5.3	31
3	56	M	I (DM)	4	90	6.1	30
4	71	M	I (DSC)	4	79	5.5	23
5	65	M	I (DL)	3	91	6.1	28
6	41	M	I (DL)*	2	81	5.5	10
7	47	M	L (FM)	4	75	5.1	7
8	42	F	L (FSC)†	3	57	3.8	8
9	56	M	H (LCI)	3	106	7.2	6
10	44	F	H (LCI)	4	71	4.8	6
11	66	F	I (DL)	3	92	6.2	6
12	41	M	I (MC)	4	88	6.1	7
13	35	M	H (LCI)*	3	67	4.8	7

*AIDS-associated NHL.
†Minimal residual disease.
I = intermediate grade; DL = diffuse large; H = high grade; LCI = large cell immunoblastic; DM = diffuse mixed; DSC = diffuse small cleaved; L = low grade; FM = follicular mixed; FSC = follicular small cleaved; MC = mantle cell.

body weight and theoretic blood volume ± SD were 80 ± 14 kg (range, 57–106 kg) and 5.4 ± 0.9 L (range, 3.8–7.1 L), respectively (*17*). Mean body surface area of the patients was 2.0 ± 0.2 m^2 (range, 1.6–2.3 m^2).

Study Design

Patients were entered into 1 of 4 trials in which the radiation dosimetry of ^{90}Y-2IT-BAD-Lym-1 was generated using ^{111}In-2IT-BAD-Lym-1 to obtain pharmacokinetic data. All patients, except 1, subsequently received therapy with radiolabeled Lym-1, so that only toxicity immediately associated with the radiopharmaceutical could be assessed. Patients were eligible if the prestudy human antimouse antibody assay (HAMA) was negative and liver function tests were within 2 times the upper limit of normal. At entry, patients had not received chemotherapy for at least 4 wk. All patients signed informed consent forms approved by the University of California at Davis human subjects and radiation use committees under an investigational new drug authorization from the U.S. Food and Drug Administration. Patients were cared for in an ambulatory center.

Pharmaceutical

Lym-1 (Techniclone, Inc., Tustin, CA, or Damon Biotechnology, Needham Heights, MA) is an IgG2a mouse MAb with high affinity against a discontinuous epitope on the β chain of the human leukocyte-DR antigen located on the surface membrane of malignant B-lymphocytes (*18,19*). Lym-1 has antibody-dependent cellular cytotoxicity and complement-dependent cytotoxicity against Raji human lymphoma cells in vitro. The hybridoma was generated by fusion of splenic lymphocytes from mice that were immunized with nuclei of cultured Raji cells originating from a patient with Burkitt's lymphoma (*19*). Lym-1 was specified as >95% pure monomeric IgG by polyacrylamide gel electrophoresis and met FDA Mouse Antibody Production guidelines for murine viral, mycoplasmatic, fungal, and bacterial contamination; endotoxin, pyrogen, and DNA content; and general safety testing in animals.

The immunoconjugate, 2IT-BAD-Lym-1, was prepared by conjugating 2-[p-(bromoacetamido)benzyl]-DOTA (BAD) to Lym-1 with 2-iminothiolane (2IT; Sigma Chemical Co., St. Louis, MO) (*20*) at final concentrations of 2.5 mmol/L, 15 mg/mL, and 1.3 mmol/L in 0.1 mol/L tetramethylammonium phosphate, pH 9, at 37°C for 30 min. The 2IT-BAD-Lym-1 conjugate was purified and transferred to 0.1 mol/L ammonium acetate, pH 5, by G50 molecular sieving chromatography (Sigma). A mean of 2.8 DOTA groups were conjugated per Lym-1 molecule.

^{111}In (0.35–1.6 GBq; Mallinckrodt, St. Louis, MO; Amersham, Arlington Heights, IL; or Nordion, Kanata, Ontario, Canada) was buffered to a final pH of 5 in 0.1 mol/L ammonium acetate, then 2IT-BAD-Lym-1 (2.4–35 mg) was added. The radiolabeling solution was incubated for 60 min at 37°C, and 0.1 mol/L sodium ethylenediamine tetraacetate (EDTA; Fisher Scientific, Pittsburgh, PA) was added to a final concentration of 10 mmol/L to scavenge nonspecifically bound ^{111}In. ^{111}In-2IT-BAD-Lym-1 was purified from ^{111}In-EDTA and transferred to 0.9% sterile saline by G25 molecular sieving chromatography (Sigma). Purified ^{111}In-2IT-BAD-Lym-1 was formulated in 4% human serum albumin/saline at 37 MBq/mL (1 mCi/mL).

^{111}In-2IT-BAD-Lym-1 was evaluated for aggregate content, radiochemical purity, and immunoreactivity by cellulose acetate electrophoresis (CAE), molecular sieving high performance liquid chromatography (HPLC), and radioimmunoreactive assay, respectively, as described (*21*).

Antibody Infusion

A preload of 5 or 20 mg Lym-1, previously shown sufficient to block nonspecific binding sites and provide stable pharmacokinetics, was given shortly before administration of 0.2 GBq (5 mCi) ^{111}In-2IT-BAD-Lym-1 (*22*). Total administered Lym-1 ranged from 6 to 31 mg and was infused at a rate of 0.5–1 mg/min (Table 1).

Toxicity

Vital signs were monitored at least every 15 min before, during, and for 2 h after Lym-1 infusion; subsequent monitoring was on a less frequent schedule. MAb-associated toxicity that occurred within 72 h of the infusion, either observed or as reported by the patient, was recorded.

Serum obtained 14–41 d after imaging from 4 patients was assayed for human antibodies reactive against Lym-1 (HAMA) or BAD (HABAD) using quantitative enzyme-linked immunoabsorbent assays (*23*).

Radiation Dosimetry

Methods for obtaining pharmacokinetic data for ^{111}In-2IT-BAD-Lym-1 have been previously described (*24*). Briefly, planar images of conjugate views were acquired immediately, at 4 h, and daily for 6–10 d after infusion of ^{111}In-2IT-BAD-Lym-1. The amount of ^{111}In in organs and tumors was quantified using geometric-mean or effective-point-source methods depending on whether the source object could be identified on both conjugate views (*24*). These methods have been validated for quantification of liver, spleen, and tumors in an abdominal phantom (*25*). Cumulated activity in tissues was obtained by fitting pharmacokinetic data to a monoexponential function, except for the blood, for which a biexponential function was used. Pharmacokinetic data for ^{90}Y-2IT-BAD-Lym-1 was assumed to be identical to that of ^{111}In-2IT-BAD-Lym-1 to derive ^{90}Y radiation dosimetry. Cumulated ^{111}In was converted to

radiation dose using the Medical Internal Radiation Dose (MIRD) formula (*26,27*). MIRD S values and reference man masses (*28*) were used for all organs except the spleen. Because of the large variation in spleen volumes in lymphoma patients, patient-specific splenic doses were determined using actual spleen volumes measured by CT images. A total of 55 tumors were identified by ^{111}In-2IT-BAD-Lym-1 imaging, of which 50 tumors with masses of at least 2 g (to ensure the accuracy of radiation dosimetry) were quantified. The radiation dose to tumor was calculated by dividing Δ_{np} by the tumor mass (*26,27*).

The radiation dose from blood to marrow was calculated as previously described (*17*):

$$D_{total} = 0.25\ \tilde{A}_{blood} \times \Delta_{np},$$

where $\tilde{A}_{blood}$ is the cumulated activity in 1 mL blood and Δ_{np} is the mean energy emitted per nuclear transition for nonpenetrating ^{90}Y emissions (*27*). The multiplier 0.25 was used to account for the difference between the specific activities of marrow and that of circulating blood (*17*).

The radiation dose to marrow was also calculated by a second method, using lumbar vertebral marrow imaging (*29*). The uptake of ^{111}In-2IT-BAD-Lym-1 in 3 lumbar vertebrae was extrapolated to uptake in total marrow, assuming that the red marrow mass in the 3 lumbar vertebrae constituted 6.7% of total red marrow mass (*30*). The extrapolated value for ^{90}Y cumulated activity in marrow and the dose-equivalent constant for nonpenetrating ^{90}Y emissions were then used to calculate the radiation dose to marrow.

Blood Clearance

Aliquots of blood obtained immediately, 2–4 h after, and daily for 6–10 d after infusion of ^{111}In-2IT-BAD-Lym-1 were assayed in a γ well counter (Pharmacia LKB, Piscataway, NJ) to obtain the concentration of ^{111}In in the blood. Cumulated ^{111}In in blood was obtained by fitting pharmacokinetic data to a biexponential function. Plasma was examined by molecular sieving HPLC (Beckman, Fullerton, CA) to assess in vivo stability of the ^{111}In-2IT-BAD-Lym-1.

Urine Clearance

All urine was collected from each patient for 6–10 d. ^{111}In was measured in aliquots of urine using a calibrated γ well counter, then multiplied by the measured urine volume to calculate daily output.

RESULTS

Thirteen patient doses were prepared from 9 lots of ^{111}In-2IT-BAD-Lym-1. Stability of the radiopharmaceutical in vitro was determined by HPLC, CAE, and immunoreactivity. The mean percentage of ^{111}In associated with 2IT-BAD-Lym-1 (±1 SD) was 99% (±2.7%) by HPLC. The mean percentage of ^{111}In-2IT-BAD-Lym-1 in monomeric form was 99% (±3.3%) by CAE. The mean immunoreactivity was 93% (±10%) relative to unmodified Lym-1.

The radiopharmaceutical showed no transfer of ^{111}In to serum proteins in vivo by molecular sieving HPLC analysis of an initial (5- to 35-min) plasma sample. Ten of 13 patients had 100% of the radioactivity as a monomeric peak with the same molecular weight as the original radiopharmaceutical; the average for the 13 patients was 92%. The blood clearance of ^{111}In-2IT-BAD-Lym-1 was biphasic; the mean biologic half-time of the blood β phase was 1.55 ± 1.90 d.

There was almost no ^{111}In in the initial 2-h urine samples, confirming the absence of free ^{111}In-BAD. Cumulative urine clearances of ^{111}In for each patient were similar to the reciprocal of total body ^{111}In determined by imaging. Mean cumulative ^{111}In excreted in urine collection intervals that ranged from 6 to 10 d (mean, 6.6) was 42 (range, 17.4–69.2) percentage injected dose (%ID).

Planar and SPECT images were of excellent quality; tumors (almost always) and normal organs were readily identified (Figs. 1–3). ^{111}In in liver, spleen, marrow, and kidneys was routinely observed; small amounts were observed in the gastrointestinal tract of most patients at 1–3 d after infusion. Tumors were usually apparent on images obtained immediately (within 0.5 h) after infusion and reached a peak uptake quantitatively by an average of 0.77 d (Table 2). By imaging, the mean peak tumor concentration was 0.018 ± 0.009 %ID/g (range, 0.004–0.036 %ID/g). Tumor uptake was not related to splenic size; for 6 patients whose spleens ranged from 309 to 2077 mL, mean peak tumor concentration was 0.016 ± 0.006 %ID/g (range,

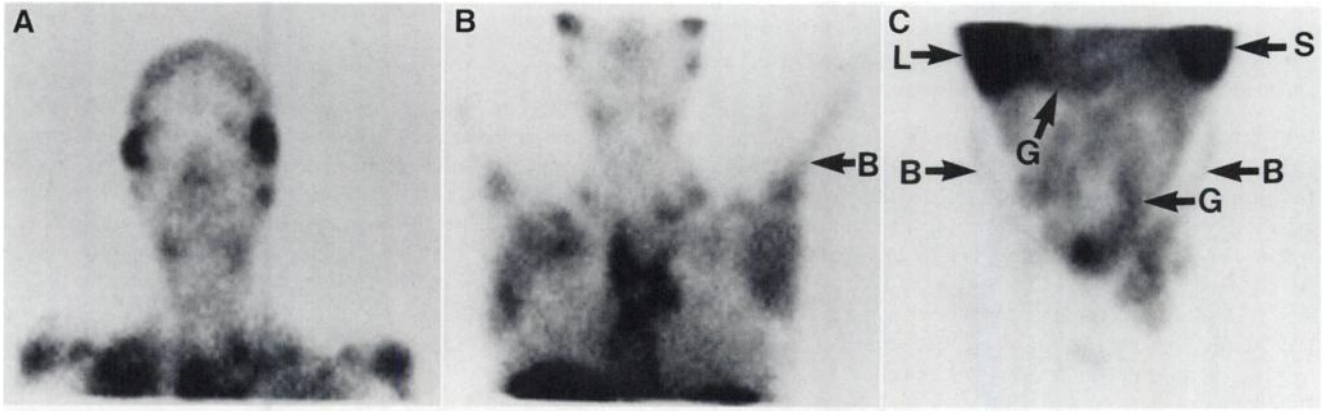

FIGURE 1. Planar anterior images of head (A), chest with arms elevated (B), and pelvis (C) obtained 2 d after infusion of 0.2 GBq ^{111}In-2IT-BAD-Lym-1 reveal multiple tumors of head, neck, and bilateral axillary, mediastinal, abdominal, and left inquinal regions. ^{111}In is also evident in marrow of pelvis and long bones (B), liver (L), spleen (S), and gastrointestinal (G) tract (arrows).

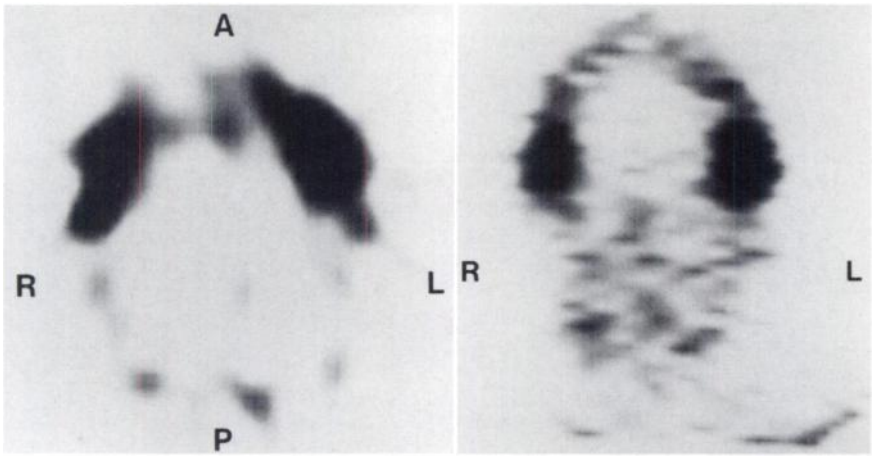

FIGURE 2. Transverse (left) and coronal (right) SPECT images (6.4-mm sections) of head obtained 2 d after infusion of ^{111}In-2IT-BAD-Lym-1 in patient shown in Figure 1 show intense uptake in tumors. (R = right; L = left; A = anterior; P = posterior [aspect of patient]).

0.008–0.027 %ID/g), whereas it was 0.020 ± 0.011 %ID/g (range, 0.009–0.036 %ID/g) for 7 patients whose spleens ranged from 281 to 0 mL (splenectomy). Biologic half-times for ^{111}In and radiation doses per unit of administered ^{90}Y were similar among patients for a specific normal tissue except for marrow data obtained by imaging 3 lumbar vertebrae (Tables 3 and 4). The biologic half-time of ^{111}In-2IT-BAD-Lym-1 in tumors was greater than the half-times of normal tissues, except for the liver, marrow (by imaging), and kidney (Table 3). The mean biologic half-time of tumors was 2.8 times longer than that of the lungs. The biologic half-time of ^{111}In in the marrow using the imaging method was variable, as has been observed for ^{131}I-Lym-1 (Table 3) (*31*). The tumor uptake of ^{111}In-2IT-BAD-Lym-1 and radiation dose from ^{90}Y-2IT-BAD-Lym-1 were greater than those values in the lung and kidney but similar to those in the liver (Table 4). The mean radiation doses to tumor, total body, lung, kidney, and liver were 6.6, 0.5, 1.4, 2.7, and 6.1 Gy/GBq (24.4, 1.8, 5.2, 10.0, and 22.6 rad/mCi), respectively. Smaller tumors received higher radiation doses than did larger tumors (Fig. 4).

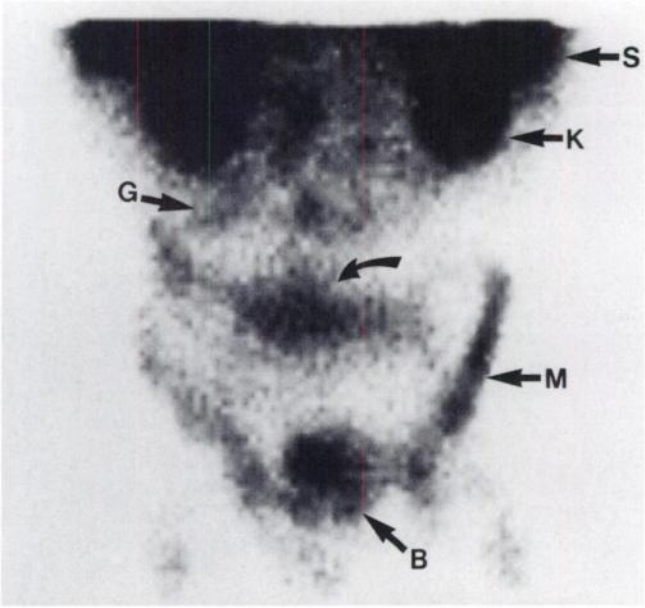

FIGURE 3. Planar anterior image of pelvis obtained 2 d after infusion of 0.2 GBq ^{111}In-2IT-BAD-Lym-1 reveals tumor (curved arrow). Substantial ^{111}In is also present in spleen (S), kidneys (K), marrow (M, asymmetric and nodular, suggesting NHL), bladder (B), and, to lesser degree, gastrointestinal (G) tract (arrows).

The mean marrow radiation dose, calculated as the nonpenetrating radiation from blood, was 0.1 Gy/GBq (0.3 rad/mCi). The mean tumor-to-marrow radiation dose ratio was 66:1 (range, 19–687:1), based on marrow radiation dose obtained by the blood method. However, the mean marrow radiation dose, obtained by lumbar vertebral imaging, was 1.5 Gy/GBq (5.5 rad/mCi). With the imaging method, marrow radiation doses were higher than those obtained with the blood method (Table 4), indicating that the latter method does not account for radiation from targeting of marrow and skeletal elements (*17,29*).

Toxicity related to Lym-1 infusion occurred in 23% (3/13) of the patients and consisted of grade 1–2 fever with chills, grade 2 nausea and vomiting, grade 1 rash, and grade 1 hypertension. The symptoms were transient. In none of the 4 patients evaluated for HAMA or HABAD were findings positive.

DISCUSSION

Longer retention of ^{111}In-labeled MAbs in the tumor, when compared with the corresponding radioiodinated MAb, was described by Halpern et al. (*32*) and subsequently was confirmed by others (*33–36*). Juweid et al. (*8*) have described strikingly improved radiation dosimetry for tumors in patients with NHL when the ^{90}Y-labeled hLL2 was compared with ^{131}I-labeled hLL2, a MAb that is highly internalized. Parker et al. (*4*) described the first patient to be treated with ^{90}Y-labeled MAb, and, subsequently, there have been several trials of ^{90}Y-labeled MAbs in hematologic malignancies (*2–8*) and solid tumors (*9–13*), sometimes in association with bone marrow transplantation (*9,13*). ^{90}Y emits β particles that have an energy and range substantially greater than those of ^{131}I. The absence of primary photon emissions means that the patient does not require hospitalization for radiation safety purposes. However, most investiga-

TABLE 2
Tissue Uptake (Immediate and Peak) of ^{111}In-2IT-BAD-Lym-1

Site	Immediate (T_0)		Peak		Time to peak (d)
	%ID	%ID/g	%ID	%ID/g	
Liver (1809 g)*	22.78 ± 6.78 (12.70–35.10)	0.013 ± 0.004 (0.007–0.019)	29.17 ± 7.19 (17.68–40.54)	0.016 ± 0.004 (0.010–0.022)	0.83 ± 0.34 (0.17–1)
Spleen (163–2077 g)†	5.83 ± 3.76 (2.66–13.08)	0.013 ± 0.005 (0.006–0.021)	7.71 ± 4.09 (3.20–14.78)	0.018 ± 0.008 (0.007–0.034)	0.88 ± 0.32 (0.17–1)
Lung (999 g)*	6.02 ± 1.17 (4.19–6.02)	0.006 ± 0.001 (0.004–0.006)	6.02 ± 1.32 (4.19–8.34)	0.006 ± 0.001 (0.004–0.008)	0
Kidney (284 g)*	1.74 ± 0.51 (0.97–2.51)	0.006 ± 0.002 (0.003–0.008)	2.01 ± 0.48 (1.38–2.75)	0.007 ± 0.002 (0.004–0.010)	0.87 ± 0.98 (0–3)
Tumor (2–293 g)‡	0.54 ± 0.49 (0.00–1.66)	0.016 ± 0.010 (0.003–0.036)	0.60 ± 0.57 (0.03–2.03)	0.018 ± 0.009 (0.004–0.036)	0.77 ± 0.53 (0–3)

*Mass for reference man from Medical Internal Radiation Dose Committee (*28*).
†Patient-specific CT mass (volume).
‡Patient-specific CT or caliper mass (volume).
Values are expressed as mean ± SD followed by range in parentheses. These and all similar statistics were generated giving equal weighting to data from each patient.

tors use ^{111}In as a surrogate for imaging and pharmacokinetic studies, because ^{90}Y has no γ emissions. ^{111}In is a suitable radionuclide for these purposes, as was observed in the study reported herein. Not all chelates bind both indium and yttrium stably. Newer chelates do provide stable radiopharmaceuticals for both ^{111}In and ^{90}Y (*1,12*). Using these chelators, ^{111}In- and ^{90}Y-labeled MAbs have been shown to have similar pharmacokinetic behavior in preclinical and clinical studies (*1,12*). Although the macrocyclic chelator DOTA was specifically synthesized for yttrium, it also stably chelates ^{111}In. The extraordinary stability of the yttrium–DOTA complex minimizes the loss of ^{90}Y to bone, a target organ of the radionuclide (*37*). DOTA-chelated ^{111}In- and ^{90}Y-labeled MAbs have been observed to have similar pharmacokinetic behavior (*12*; G Denardo, unpublished data, 1998), thereby justifying the use of ^{111}In-2IT-BAD-Lym-1 to obtain radiation dosimetry for ^{90}Y-2IT-BAD-Lym-1 in our study.

TABLE 3
Pharmacokinetics (Biologic Half-Time [d]) of ^{111}In-2IT-BAD-Lym-1 Determined Using Monoexponential Analysis

Patient	Body	Blood*		Marrow†	Liver	Spleen	Lung	Kidney	Tumors (n)
		α	β						
1	7.6	0.02	0.34	‡	8.5	7.6	4.5	9.3	7.5, 8.2 (2)
2	8.2	0.08	0.89	2.6	8.7	8.4	3.4	7.0	5.3–15.4 (12)
3	7.1	0.04	7.55	13.8	9.5	5.2	4.8	12.8	18.6, 18.9 (2)
4	8.2	0.31	2.81	‡	21.6	12.7	3.1	10.8	9.2–18.9 (5)
5	6.8	0.01	0.47	1.5	8.1	7.6	4.2	6.9	10.0 (1)
6	8.1	0.09	0.91	16.6	6.7	9.2	7.0	8.0	10.5, 14.4 (2)
7	7.2	0.10	0.96	14.0	8.0	7.0	3.2	7.9	4.2–19.6 (10)
8	10.4	0.13	1.21	12.2	10.5	9.4	2.4	18.4	§
9	5.4	0.16	0.67	‡	10.3	6.5	3.1	10.7	7.7, 14.9 (2)
10	6.9	0.15	0.69	‡	‡	10.4	2.5	8.3	4.1 (1)
11	6.9	0.57	2.34	13.1	‡	‡	3.0	‡	10.1 (1)
12	6.4	0.02	0.04	7.7	8.3	‖	3.1	‡	6.2–20.0 (11)
13	7.2	0.08	1.29	9.1	8.5	5.8	3.8	22.7	6.0 (1)
Mean	7.4	0.14	1.55	10.1	9.9	8.2	3.7	11.2	10.3
SD	1.4	0.15	1.90	5.3	4.0	2.2	1.4	5.1	3.8
Range	5.4–10.4	0.01–0.57	0.04–7.55	1.5–16.6	6.7–21.6	5.2–12.7	2.4–7.0	6.9–22.7	4.1–20.0

*Blood α and β half-times.
†Marrow determined by imaging 3 lumbar vertebrae.
‡Use of monoexponential fit was not appropriate because concentration increased over time.
§Patient had no tumor that fulfilled the criteria for accurate quantification.
‖Splenectomy.

TABLE 4
Tissue Radiation Doses (Gy/GBq) from ^{90}Y-2IT-BAD-Lym-1 Using ^{111}In-2IT-BAD-Lym-1 Pharmacokinetic Data

Patient	Body	Marrow*	Marrow†	Liver	Spleen	Lung	Kidney	Tumors (n)
1	0.54	0.08	2.79	4.54	5.24	1.42	2.47	2.13, 3.66 (2)
2	0.49	0.15	0.33	4.89	4.35	1.50	2.35	2.24–8.29 (12)
3	0.54	0.03	0.75	7.51	2.48	1.43	3.52	1.97, 6.25 (2)
4	0.56	0.21	2.18	4.40	3.08	1.80	3.00	4.36–9.21 (5)
5	0.53	0.02	‡	6.43	7.75	1.24	3.39	10.99 (1)
6	0.51	0.05	1.85	3.66	2.81	1.16	1.21	12.99, 13.85 (2)
7	0.51	0.04	0.79	6.24	4.67	1.37	3.39	3.94–7.76 (10)
8	0.53	0.11	1.52	5.79	8.02	1.51	3.27	§
9	0.47	0.11	1.27	7.92	5.77	1.34	1.96	4.46, 6.57 (2)
10	0.50	0.14	3.53	7.43	11.37	1.33	2.23	9.72 (1)
11	0.50	0.31	1.44	6.40	8.16	1.29	2.65	6.00 (1)
12	0.51	0.04	1.68	6.08	‖	1.43	1.89	2.08–8.06 (11)
13	0.52	0.03	1.39	8.18	6.78	1.02	3.73	3.26 (1)
Mean	0.52	0.10	1.50	6.10	5.89	1.37	2.70	6.57
SD	0.02	0.09	0.89	1.43	2.65	0.19	0.76	3.18
Range	0.47–0.56	0.02–0.31	0.33–3.53	3.67–8.18	2.48–11.37	1.02–1.80	1.22–3.73	1.97–13.85

*Marrow dose from blood cumulated activity and assuming 25% of marrow space is blood.
†Marrow dose determined by imaging 3 lumbar vertebrae to obtain cumulated activity.
‡Lumbar retroperitoneal radiotherapy 4.5 Gy within a year.
§Patient had no tumor that fulfilled criteria for accurate dosimetry.
‖Splenectomy.

Because ^{111}In provided good definition of tumors and organs, the resulting pharmacokinetic data were assumed to be of good quality. To the extent that the pharmacokinetics of ^{111}In-2IT-BAD-Lym-1 reflect those of ^{90}Y-2IT-BAD-Lym-1, several of the therapeutic ratios (tumor-to-normal tissue) were less favorable than those observed for ^{131}I- (*31*) or ^{67}Cu-labeled (*21*) Lym-1. Although ^{111}In was retained in the tumors, it was also retained in the liver, where there was little therapeutic advantage based on the relative ratio of the tumor-to-liver dosimetry; another group has reported similar observations (*38*). However, all of the therapeutic indices, including tumor-to-liver, are greater if only tumors <25 g in size are considered (Fig. 4). Greater certainty on the relevance of these observations for ^{90}Y-MAb RIT must await the availability of yttrium radionuclides that have been suggested for imaging (^{86}Y, ^{87}Y) (*39,40*). A novel ^{111}In/^{90}Y-labeled MAb with a glycylglycylglycyl-L-phenylalanine linker between the MAb and the DOTA chelator has been shown to reduce the liver radiation dose when compared with the same radiopharmaceutical containing the 2IT linker (*41*). The novel peptide linker was designed to be biodegradable by intrahepatocyte cathepsins, with the rationale that this would facilitate cleavage and excretion of the radiochelate.

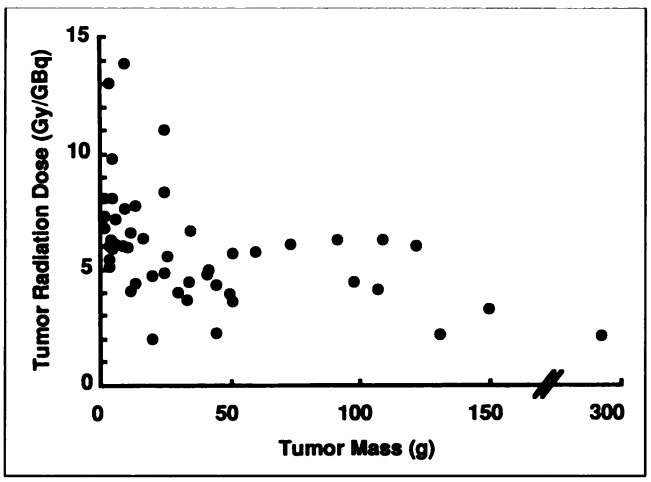

FIGURE 4. Comparison of tumor size and radiation dose from ^{90}Y-2IT-BAD-Lym-1. Radiation dose was calculated using pharmacokinetic data obtained after infusion of ^{111}In-2IT-BAD-Lym-1. Radiation dose was higher for smaller tumors. Tumors ranged in size from 2 to 293 g.

CONCLUSION

Using ^{111}In-2IT-BAD-Lym-1 pharmacokinetic data as a surrogate, the therapeutic ratios for ^{90}Y-2IT-BAD-Lym-1 do not uniformly suggest that this radiopharmaceutical is superior to ^{131}I- or ^{67}Cu-labeled Lym-1. Retention of ^{90}Y in the liver, observed by other investigators for other MAbs as well, may cause this organ to be dose limiting in high-dose, myeloablative strategies.

ACKNOWLEDGMENTS

The authors thank Desiree Goldstein and Qansy Salako for assistance with data assembly and radiopharmaceutical preparation. This study was supported by National Cancer Institute grants PO1 CA47829 and PHS CA16861 and by Department of Energy grant DE FG03-84ER60233.

REFERENCES

1. Carrasquillo JA, White JD, Paik CH, et al. Similarities and differences in ^{111}In- and ^{90}Y-labeled 1B4M-DTPA antiTac monoclonal antibody distribution. *J Nucl Med.* 1999;40:268–276.
2. Knox SJ, Goris ML, Trisler K, et al. Yttrium-90-labeled anti-CD20 monoclonal antibody therapy of recurrent B-cell lymphoma. *Clin Cancer Res.* 1996;2:457–470.
3. White CA, Halpern SE, Parker BA, et al. Radioimmunotherapy of relapsed B-cell lymphoma with yttrium 90 anti-idiotype monoclonal antibodies. *Blood.* 1996;87:3640–3649.
4. Parker BA, Vassos AB, Halpern SE, et al. Radioimmunotherapy of human B-cell lymphoma with Y-90-conjugated antiidiotype monoclonal antibody. *Cancer Res.* 1990;50:1022–1028.
5. Bierman PJ, Vose JM, Leichner PK, et al. Yttrium 90-labeled antiferritin followed by high-dose chemotherapy and autologous bone marrow transplantation for poor-prognosis Hodgkin's disease. *J Clin Oncol.* 1993;11:698–703.
6. Waldmann TA, White JD, Carrasquillo JA, et al. Radioimmunotherapy of interleukin-2R-alpha-expressing adult T-cell leukemia with yttrium-90-labeled anti-Tac. *Blood.* 1995;86:4063–4075.
7. Vriesendorp HM, Morton JD, Quadri SM. Review of five consecutive studies of radiolabeled immunoglobulin therapy in Hodgkin's disease. *Cancer Res.* 1995;55 (suppl):5888S–5892S.
8. Juweid ME, Stadtmauer E, Sharkey RM, et al. Pharmacokinetics, dosimetry and initial therapeutic results with ^{131}I- and ^{111}In-/^{90}Y-labeled humanized LL2 anti-CD22 monoclonal antibody in patients with relapsed/refractory non-Hodgkin's lymphoma. *Clin Cancer Res.* 1999;5:3292–3303.
9. Schrier DM, Stemmer SM, Johnson T, et al. High-dose ^{90}Y Mx-diethylenetriamine-pentaacetic acid (DTPA)-BrE-3 and autologous hematopoietic stem cell support (AHSCS) for the treatment of advanced breast cancer: a phase I trial. *Cancer Res.* 1995;55(suppl):5921S–5924S.
10. Wong JY, Williams LE, Yamauchi DM, et al. Initial experience evaluating ^{90}Y-radiolabeled anti-carcinoembryonic antigen chimeric T84.66 in a phase I radioimmunotherapy trial. *Cancer Res.* 1995;55:5929–5934.
11. DeNardo SJ, Kramer EL, O'Donnell RT, et al. Radioimmunotherapy for breast cancer using indium-111/yttrium-90 BrE-3: results of a phase I clinical trial. *J Nucl Med.* 1997;38:1180–1185.
12. DeNardo SJ, Richman CM, Goldstein DS, et al. Yttrium-90/indium-111-DOTA-peptide-chimeric L6: pharmacokinetics, dosimetry and initial results in patients with incurable breast cancer. *Anticancer Res.* 1997;17:1735–1744.
13. Richman CM, DeNardo SJ, O'Donnell RT, et al. Dosimetry-based therapy in metastatic breast cancer patients using ^{90}Y Mab 170H.82 with autologous stem cell support and cyclosporin A. *Clin Cancer Res.* 1999;5:3243–3248.
14. Moi MK, Meares CF, DeNardo SJ. The peptide way to macrocyclic bifunctional chelating agents: synthesis of 2-(p-nitrobenzyl)-1,4,7,10-tetraazacyclododecane -N,- N′,N″,N‴-tetraacetic acid and study of its yttrium (III) complex. *J Am Chem Soc.* 1988;110:6266–6267.
15. Moi MK, DeNardo SJ, Meares CF. Stable bifunctional chelates of metals used in radiotherapy. *Cancer Res.* 1990;50(suppl):789–793.
16. The Non-Hodgkin's Lymphoma Pathologic Classification Project. National Cancer Institute sponsored study of classifications of non-Hodgkin's lymphomas: summary and description of a working formulation for clinical usage. *Cancer* 1982;49:2112–2135.
17. DeNardo GL, Mahe MA, DeNardo SJ, et al. Body and blood clearance and marrow radiation dose of ^{131}I-Lym-1 in patients with B-cell malignancies. *Nucl Med Commun.* 1993;14:587–595.
18. Rose LM, Gunasekera AH, DeNardo SJ, DeNardo GL, Meares CF. Lymphoma-selective antibody Lym-1 recognizes a discontinuous epitope on the light chain of HLA-DR10. *Cancer Immunol Immunother.* 1996;43:26–30.
19. Epstein AL, Marder RJ, Winter JN, et al. Two new monoclonal antibodies, Lym-1 and Lym-2, reactive with human-B-lymphocytes and derived tumors, with immunodiagnostic and immunotherapeutic potential. *Cancer Res.* 1987;47:830–840.
20. McCall MJ, Diril H, Meares CF. Simplified method for conjugating macrocyclic bifunctional chelating agents to antibodies via 2-iminothiolane. *Bioconjug Chem.* 1990;1:222–226.
21. DeNardo SJ, DeNardo GL, Kukis DL, et al. ^{67}Cu-2IT-BAT-Lym-1 pharmacokinetics, radiation dosimetry, toxicity and tumor regression in patients with lymphoma. *J Nucl Med.* 1999;40:302–310.
22. DeNardo GL, DeNardo SJ, O'Grady LF, Levy NB, Adams GP, Mills SL. Fractionated radioimmunotherapy of B-cell malignancies with ^{131}I-Lym-1. *Cancer Res.* 1990;50(suppl):1014–1016.
23. DeNardo GL, Mirick GR, Kroger LA, O'Donnell RT, Meares CF, DeNardo SJ. Antibody responses to macrocycles in lymphoma. *J Nucl Med.* 1996;37:451–456.
24. Erwin WD, Groch MW, Macey DJ, DeNardo GL, DeNardo SJ, Shen S. A radioimmunoimaging and MIRD dosimetry treatment planning program for radioimmunotherapy. *Nucl Med Biol.* 1996;23:525–532.
25. Shen S, DeNardo GL, DeNardo SJ, Yuan A, DeNardo DA, Lamborn KR. Reproducibility of operator processing for radiation dosimetry. *Nucl Med Biol.* 1997;24:77–83.
26. Loevinger R, Berman M. *A Revised Schema for Calculating the Absorbed Dose from Biologically Distributed Radionuclides. MIRD Pamphlet No. 1.* New York, NY: Society of Nuclear Medicine; 1976:1–10.
27. Dillman LT. *Radionuclide Decay Schemes and Nuclear Parameters for Use in Radiation-Dose Estimation. Part 2. MIRD Pamphlet No. 6.* New York, NY: Society of Nuclear Medicine; 1970:5–32.
28. Snyder WS, Ford MR, Warner GG. *"S" Absorbed Dose per Unit Cumulated Activity for Selected Radionuclides and Organs. MIRD Pamphlet No. 11.* New York, NY: Society of Nuclear Medicine; 1975:82–83.
29. Lim S-M, DeNardo GL, DeNardo DA, et al. Prediction of myelotoxicity using radiation doses to marrow from body, blood and marrow sources. *J Nucl Med.* 1997;38:1374–1378.
30. Brodsky A. *CRC Handbook of Radiation Measurements and Protection, Section A. Volume II: Biological and Mathematical Information.* West Palm Beach, FL: CRC Press, 1982:148–150.
31. DeNardo GL, DeNardo SJ, DeNardo DA, et al. Factors affecting ^{131}I-Lym-1 pharmacokinetics and radiation dosimetry in patients with non-Hodgkin's lymphoma (NHL) and chronic lymphocytic leukemia. *J Nucl Med.* 1999;40:1317–1326.
32. Halpern SE, Hagan PL, Garver PR, et al. Stability, characterization, and kinetics of ^{111}In-labeled monoclonal antitumor antibodies in normal animals and nude-mouse human tumor models. *Cancer Res.* 1983;43:5347–5355.
33. Stein R, Juweid M, Mattes MJ, Goldenberg DM. Carcinoembryonic antigen as a target for radioimmunotherapy of human medullary thyroid carcinoma: antibody processing, targeting and experimental therapy with ^{131}I and ^{90}Y labeled MAbs. *Cancer Biother Radiopharm.* 1999;14:37–47.
34. Stein R, Chen S, Haim S, Goldenberg DM. Advantage of yttrium-90-labeled over iodine-131-labeled monoclonal antibodies in the treatment of a human lung carcinoma xenograft. *Cancer.* 1997;80(suppl):2636–2641.
35. Sharkey RM, Motta-Hennessy C, Pawlyk D, Siegel JA, Goldenberg DM. Biodistribution and radiation dose estimates for yttrium- and iodine-labeled monoclonal antibody IgG and fragments in nude mice bearing human colonic tumor xenografts. *Cancer Res.* 1990;50:2330–2336.
36. DeNardo SJ, Zhong G-R, Salako Q, Li M, DeNardo GL, Meares CF. Pharmacokinetics of chimeric L6 conjugated to indium-111 and yttrium-90-DOTA-peptide in tumor bearing mice. *J Nucl Med.* 1995;36:829–836.
37. DeNardo GL, Kroger LA, DeNardo SJ, et al. Comparative toxicity studies of yttrium-90 MX-DTPA and 2-IT-BAD conjugated monoclonal antibody (BrE-3). *Cancer.* 1994;73:1012–1022.
38. Sharkey RM, Blumenthal RD, Behr TM, et al. Selection of radioimmunoconjugates for the therapy of well-established or micrometastatic colon carcinoma. *Int J Cancer.* 1997;72:477–485.
39. Sgouros G. Yttrium-90 biodistribution by yttrium-87 imaging: a theoretical feasibility analysis. *Med Phys.* 1998;25:1487–1490.
40. Rosch F, Herzog H, Plag C, et al. Radiation doses of yttrium-90 citrate and yttrium-90 EDTMP as determined via analogous yttrium-86 complexes and positron emission tomography. *Eur J Nucl Med.* 1996;23:958–966.
41. DeNardo GL, Kroger LA, Meares CF, et al. Comparison of DOTA-peptide-ChL6, a novel immunoconjugate with catabolizable linker, to 2IT-BAD-ChL6 in breast cancer xenografts. *Clin Cancer Res.* 1998;4:2483–2490.